DATA DRIVEN MODEL DEVELOPMENT FOR THE SUPERSONIC SEMISPAN TRANSPORT (S^4T)

Sunil L. Kukreja[1]

[1]NASA, Dryden Flight Research Center

Edwards, California, USA

Sunil.Kukreja@nasa.gov

Keywords: aeroelasticity, system identification, data driven modelling, S^4T, aircraft safety, gust-load alleviation, ride quality

Abstract: We investigate two common approaches to model development for robust control synthesis in the aerospace community; namely, reduced order aeroservoelastic modelling based on structural finite-element and computational fluid dynamics based aerodynamic models and a data-driven system identification procedure. It is shown via analysis of experimental Super-Sonic SemiSpan Transport (S^4T) wind-tunnel data using a system identification approach it is possible to estimate a model at a fixed Mach, which is parsimonious and robust across varying dynamic pressures.

1 INTRODUCTION

Undesirable aeroservoelastic (ASE) interactions are a major concern in modern aircraft design. ASE interactions between aircraft structure, aerodynamics and flight control systems can lead to divergent oscillations resulting in catastrophic failure [1]. As such, analytical model development is an important step in the design and certification of aircraft. Accurate models allow for robust control design, which is critical for aircraft safety, gust-load alleviation, ride quality, etc.

Finite element (FE) based models are used in the design process of aircraft to aid in the description of complex elastic and structural components [2, 3]. FE based models that accurately characterise the aerodynamic and structural components are of very high order (e.g. thousands of degrees of freedom) and computationally intensive. To reduce the ASE model order a modal approach is used. This can reduce the state-space model order to several tens of states. The robustness of this model type highly depends on the accuracy of the FE structural and aerodynamic models and on the number of states applied to the modelling. Models of high complexity

inhibit their use for control synthesis because their real-time implementation is difficult or not possible [4]. This difficulty has led to considerable activity in the areas of model and controller reduction techniques in the last decade. The literature is rich with many reduced order model (ROM) techniques which would require a review paper to properly discuss them. As such, in this paper, we limit ourselves to a handful of approaches.

A leading strategy to FE based model reduction is the proper orthogonal decomposition (POD), which is also known as the Karhunen-Loeve procedure [5]. The so-called POD technique is well known in the statistical literature as principal-component analysis [6]. The reduced basis method was first proposed in [7, 8] for structural analysis and it has been used for structural problems in [9–11]. This technique uses synthetic data from a high fidelity FE based model to capture the dominant characteristic information utilising an orthogonalisation process. This allows the POD approach to accurately describe a system using a few basis terms, which gives it an advantage compared to other numerical procedures [12]. These reasons have allowed POD to become a popular technique for the implementation of real-time control [13]. Moreover, it has been successfully used in a variety of fields including signal analysis and pattern recognition [14], fluid dynamics and coherent structures [15–17], control theory [18–20], civil engineering [21] and inverse problems [22].

More recently the ROM techniques utalising POD were developed for aeroelastic systems analysis [23]. This methodology was introduced to the aerospace community for the reduction of aeroelastic equations [24]. As a follow-on to this technique, frequency-domain approaches were developed which efficiently compute POD basis functions for linearised aeroelastic systems [25, 26]. Due to its popularity and utility POD methodology has been proposed and implemented for static and dynamic continuous-time nonlinear aeroelastic problems. Subsequent development lead to extensions to encompass discrete Euler equations [27, 28]. Successful application of this approach has been demonstrated for the analysis of limit-cycle oscillation of an airfoil with a nonlinear structural coupling in the transonic regime [29].

Nevertheless, it has been observed that standard POD procedures are less robust for nonlinear problems and typically require more basis functions as the function complexity increases [23, 30]. To address this limitation a linearisation strategy, the trajectory piecewise linearisation (TPWL), was proposed [31, 32]. The TPWL technique combines reduced-order modelling with linearization of the governing equations as a solution to this problem [23].

Although POD offers a significant reduction of the full FE based model, it is often too large to lend itself to efficient control design. An alternative approach is to use data driven techniques to let the data dictate what the optimal model should be. Such a procedure is commonly known as system identification.

This area, as with ROM methods, also has an extensive base of literature for both linear and nonlinear system identification techniques and is too large to give a proper review here. As such we refer the reader to an often cited authoritative treatise in the area which provides an excellent overview and references [33]. Below we provide a brief and incomplete introduction.

There are two broad classes of techniques that can be pursued to accomplish the task of system identification: (i) nonparametric and (ii) parametric methods. The finite impulse response function (FIR) has been widely used for modelling linear time-invariant systems. This type of system description is known as nonparametric because it is a numeric representation of the system's impulse response or kernel [33–35]. Although nonparametric methods can be used to represent many classes of systems, they do so at the expense of introducing an excessive number of unknown coefficients which must be estimated. Most expansions map the past inputs into the present output and so require a very large number of coefficients to characterize the process. Moreover, the parameters are not readily linked to the underlying system, except in special cases where significant *a priori* knowledge of the system has been assumed.

Due to this shortcoming, parametric identification methods have been developed for use in the design of better control systems. Parametric models have some advantages in applications. They (i) are easier to understand and interpret, (ii) can simplify forecasts (e.g., obtaining forecast intervals) and (iii) model comparison in a parametric context (i.e., parameter estimates, model order and model structure) has been well studied. Hence, the difficulty of model comparison encountered using nonparametric tools can be avoided [36].

A parametric model consists of a set of differential or difference equations describing the system dynamics. Such equations usually contain a "small" number of parameters which can be varied to alter the behavior of the equation. In this paper, we only consider the discrete-time case since in any practical experimental situation the data available to the experimenter is in discrete-time. As such, most systems for identification purposes are represented in discrete-time. In addition, we assume the ROM with which we compare our data-driven model is available and as such we

do not discuss its development.

The organization of this paper is as follows. In §2 we formulate the identification problem addressed here. Section 3 describes the experimental S^{4}T test-bed [37] and methods used for model development. Section 4 illustrates the results of our study on three flight conditions; namely, model robustness to fixed Mach but varying dynamic pressure. Section 5 provides a discussion of our findings and §6 summarises the conclusions of our study.

2 PROBLEM STATEMENT

System identification is the process of developing or improving a mathematical representation of a physical system based on observed data. Often the observed data consists of an external user selected input, used to perturb the system and elicit an output response. In any experimental situation the system output is a sum of the true unknown system output and observation or measurement noise. Given this paradigm there are several model structures that can be explored to model a system's dynamics and noise.

2.1 Model Structures

After preprocessing the recorded data, the first step in system identification is to select a model structure to describe the observations. There are a number of model forms to select from when developing a data-driven model [33]. However, the problem often dictates the model form(s) that are reasonable to consider. This insight may come from *a priori* knowledge of the physical process or previous morphological modelling efforts. In this paper, we use knowledge gained from previous work to limit the model sets considered, namely, linear, time-invariant processes where both input-ouput are available to the user [38, 39].

2.1.1 ARX Model Structure

The simplest input-output polynomial model is the AutoRegressive eXogenous input (ARX) model, represented as [33, 40, 41]

$$\begin{aligned} y(n) = \quad & - \quad a_1 y(n-1) - \cdots - a_{n_a} y(n-n_a) \\ & + \quad b_1 u(n-1) + b_2 u(n-2) + \cdots + b_{n_b} u(n-n_b) \\ & + \quad e(n) \end{aligned} \tag{1}$$

where $y(n)$ is the measured output, $u(n)$ is an accessible input, and $e(n)$ is an unobservable white-noise disturbance. The current output depends on n_b previous values of the input, n_a previous values of the output and the current disturbance.

This structure can be represented more compactly as

$$A(q)y(n) = B(q)u(n) + e(n) \quad \text{or} \tag{2}$$

$$y(n) = G(q)u(n) + H(q)e(n) \quad \text{where} \tag{3}$$

$$G(q) = \frac{B(q)}{A(q)}, \quad H(q) = \frac{1}{A(q)} \tag{4}$$

where $A(q) = 1 + a_1 q^{-1} + \cdots + a_{n_a} q^{-n_a}$, $B(q) = b_1 q^{-1} + \cdots + b_{n_b} q^{-n_b}$, q^{-1} is the backward shift operator and the a's and b's are the parameters of the output and input, respectively.

When there is evidence of significant noise in the system a more flexible noise model may be required to model the dynamics and noise using different polynomials.

2.1.2 ARMAX Model Structure

For linear systems, the relationship between input-output and noise can be written as a linear difference equation

$$\begin{aligned} y(n) = \quad & - \quad a_1 y(n-1) - \cdots - a_{n_a} y(n-n_a) \\ & + \quad b_1 u(n-1) + b_2 u(n-2) + \cdots + b_{n_b} u(n-n_b) \\ & + \quad e(n) + c_1 e(n-1) + \cdots + c_{n_c} e(n-n_c). \end{aligned} \tag{5}$$

This is known as the AutoRegressive, Moving Average eXogenous (ARMAX) model. In this model structure the current output $y(n)$ depends on an exogenous input, $u(n)$, an innovation process, $e(n)$, and past values of the output. This structure can be represented more compactly as

$$A(q)y(n) = B(q)u(n) + C(q)e(n). \tag{6}$$

Substituting (6) into (3) yields

$$G(q) = \frac{B(q)}{A(q)}, \quad H(q) = \frac{C(q)}{A(q)} \tag{7}$$

where $C(q) = 1 + c_1 q^{-1} + \cdots + c_{n_c} q^{-n_c}$, and the c's are parameters of the noise model numerator. The extra polynomial, $C(q)$, gives the ARMAX structure additional flexibility to model additive disturbance. When additional complexity is needed to model noise $H(q)$ can be fully parameterised independent of the system dynamics.

2.1.3 Box-Jenkins Model Structure

A natural development of the ARMAX model structure is to parameterise the noise process as an ARMA model

$$y(n) = \frac{B(q)}{F(q)} u(n) + \frac{C(q)}{D(q)} e(n) \tag{8}$$

where $F(q) = 1 + f_1 q^{-1} + \cdots + f_{n_f} q^{-n_f}$ and $D(q) = 1 + d_1 q^{-1} + \cdots + d_{n_d} q^{-n_d}$ model the poles of the system and noise separately. Note that $n_f = n_a$. This model structure is known as the Box-Jenkins model due to their seminal work proposing this model form [42].

2.2 Model Order Selection

Once a model structure is selected the dynamic order of the system needs to be determined. Although there are many techniques that offer a solution to this problem, below we describe three commonly used techniques to estimate model order.

2.2.1 Final Prediction Error

The Final Prediction Error (FPE) measure estimates the error in model fit when it is used to predict new outputs [43]. FPE defines an optimal model as one that minimises

$$\text{FPE} = V \left(1 + \frac{2p}{N - p} \right) \tag{9}$$

where N is the number of data points, V is the prediction error, or the residual sum of squares and p is the number of model parameters.

2.2.2 Akaike's Information Criterion

Akaike's Information Criterion (AIC) is a weighted estimation error based on the unexplained variation of a given time series with a penalty term when exceeding the optimal number of

parameters to represent the system [44]. Utalisng AIC, an optimal model is defined as one that minimises

$$\text{AIC} = V\left(1 + \frac{2p}{N}\right). \tag{10}$$

According to Akaike's theory, the most accurate model has the smallest prediction error.

2.2.3 Minimal Description Length

Rissanen's Minimal Description Length (MDL) approach is based on V plus a penalty for the number of terms used [45]. With MDL, an optimal model is one that minimises

$$\text{MDL} = V\left(1 + \frac{p \ln N}{N}\right). \tag{11}$$

A model that minimises the MDL allows the shortest description of measured data.

2.3 Cross-Validation

Model validation is an important step in developing strategies for robust control. This step is typically preceded by system identification. Model validation is concerned with assessing whether a given nominal model can reproduce data from a plant, collected after some initial experiments to obtain estimation data [46]. The model validation problem is really one of model invalidation since a given model can only be said to be not invalidated with the current evidence. Future evidence may invalidate the model.

We cross-validate the parameter estimates of the model dynamics using a 1-step-ahead predictor [33]. Model goodness is assessed by computing the percent quality of fit (%QF) as

$$\%QF \;=\; \left(1 - \frac{\frac{1}{N}\sum_{n=1}^{N}(y_n - \hat{y}_n)^2}{\frac{1}{N}\sum_{n=1}^{N}(y_n)^2}\right) \times 100 \tag{12}$$

where y is the measured system output and $\hat{y}$ the predicted model output.

In the sequel, we show by implementing these well-known identification strategies it is possible to develop a model which is parsimonious and a robust predictor of measured data and, hence, represent the physical process more accurately.

Figure 1: S^{4}T model.

3 EXPERIMENTAL S^{4}T WIND-TUNNEL DATA

The modelling and identification techniques were applied to experimental wind-tunnel data from the S^{4}T project conducted at NASA Langely Research Center [37]. Figure 1 shows a scale model of the S^{4}T testbed in the wind tunnel. The data analysed for this study used horizontal tail position input and structural accelerometer response output.

3.1 Data Collection

Wind-tunnel data was gathered during transonic clearance of the S^{4}T. At each flight condition the aircraft model was perturbed with a log sine sweep input which had a frequency content of 0.5–25 Hz, mean value of 3.5 deg and ± 0.3 deg amplitude. The inputs were applied to the horizontal tail. The accelerometer output was collected from a sensor located at the nacelle inboard aft position. Wind-tunnel tests were conducted at subsonic, transonic and supersonic conditions and varying dynamic pressures. The input-output were antialiasing filtered by an eighth-order Bessel filter with a cut-off at 200 Hz and recorded at 1,000 Hz. Data was collected for a range of Mach numbers from $M = 0.6 - 1.2$ and dynamic pressures $Q = 20 - 65$ psf (pounds per square foot).

3.2 Data Analysis

In this study, the objective was to develop a parsimonious model for control synthesis to improve gust-load alleviation and ride quality. As such, we focused our identification efforts on data collected at Mach 0.80, 0.95, 1.10 and $Q = 30$, 55, 60, 65 psf. At each Mach we used $Q = 30$ psf as the estimation data and $Q = 55, 60, 65$ psf as the cross-validation data. At $M = 0.95$ data was not collected at $Q = 65$ psf and, therefore, the estimated model could only be cross-validated at $Q = 55$ and 60 psf. This approach of modelling and validation was taken to assess the model's predicative capability and robustness.

Data was preprocessed to remove the linear trend, mean and outliers. The preprocessing step ensured that all unwanted low-frequency disturbances, offsets, trends and drifts were removed and allowed for an accurate representation of the system dynamics.

3.3 Identification Procedures

The identification process was performed in four stages to assess the full range of models discussed in §2. In all cases the model order was estimated using the FPE, AIC and MDL approaches. The optimal model order was deemed as one that produced the lowest prediction error of the aforementioned techniques. Once the model order was fixed, prediction error identification (PEI) was used to estimate the unknown parameters and its predictive capability was computed for a cross-validation set as described previously (see §2.3).

1. The ARX structure's ability to model wind-tunnel data was assessed because it is the simplest input-output model and invoking the principle of parsimony. For the ARX model the order was determined by preselecting a range of model orders to search over. Specifically, n_a =2–5, n_b =1–5 and n_k =1–10 was chosen as the search range, where n_k denotes input delay. This range was selected to allow sufficient model complexity whilst maintaining an efficient system description.
2. Further complexity was added to the ARX model to assess whether the same model structure could account for significantly greater output variance with n_a =2–10, n_b =1–10 and n_k =1–20.
3. Using the best fit ARX model order to fix n_a and n_b we searched for an ARMAX order, namely, n_c =1–20 that provided the smallest prediction error as the optimal ARMAX order.

4. The same procedure was followed to assess whether the BJ model structure could account for more of the output variance than the ARMAX model with n_d =1–20.

4 RESULTS

4.1 ARX Model

Two ARX model orders were evaluated. Specifically, a model with order n_a =5, n_b =1, n_k =1 and n_a =10, n_b =1, n_k =1 was used for model development. The model order was estimated as discussed in §2.2. This analysis allowed for us to assess whether adding complexity to the same structure could account for significantly more of the output variance. The models were estimated using wind-tunnel data measured at Mach1.10, $Q = 30$ psf which yielded structures of the form

$$
\begin{aligned}
&\text{ARX5:} \\
\hat{A}(q)y(n) &= \hat{B}(q)u(n) + e(n) \quad \text{where} \qquad (13)\\
\hat{A}(q) &= 1 + \hat{a}_1 q^{-1} + \hat{a}_2 q^{-2} + \hat{a}_3 q^{-3} + \hat{a}_4 q^{-4} + \hat{a}_5 q^{-5} \quad \text{and} \\
\hat{B}(q) &= \hat{b}_1 q^{-1} \\
&\text{ARX10:} \\
\tilde{A}(q)y(n) &= \tilde{B}(q)u(n) + e(n) \quad \text{where} \qquad (14)\\
\tilde{A}(q) &= 1 + \tilde{a}_1 q^{-1} + \tilde{a}_2 q^{-2} + \tilde{a}_3 q^{-3} + \tilde{a}_4 q^{-4} + \tilde{a}_5 q^{-5} \\
&+ \tilde{a}_6 q^{-6} + \tilde{a}_6 q^{-6} + \tilde{a}_6 q^{-6} + \tilde{a}_6 q^{-6} + \tilde{a}_{10} q^{-10} \quad \text{and} \\
\tilde{B}(q) &= \tilde{b}_1 q^{-1}.
\end{aligned}
$$

Figure 2 shows representative results for the ARX structure's (Eqns.13 &14) ability to represent S^{4}T wind-tunnel data by evaluating it with cross-validation data at Mach 1.10, Q =55, 60, 65 psf. This figure compares %QF of the predicted output for the ARX5 and ARX10 models superimposed on top of measured data. The %QF's obtained for the ARX5 model at Q =55, 60, 65 psf. are 82.97%, 84.94% and 84.94%, respectively. For the ARX10 model the %QF's are 86.61%, 88.24% and 88.05%.

Figure 2 demonstrates that adding complexity to the ARX model improves the %QF. As such, we deem that the ARX10 model (Eqn. 14) is the better fit model due to its predicative capability.

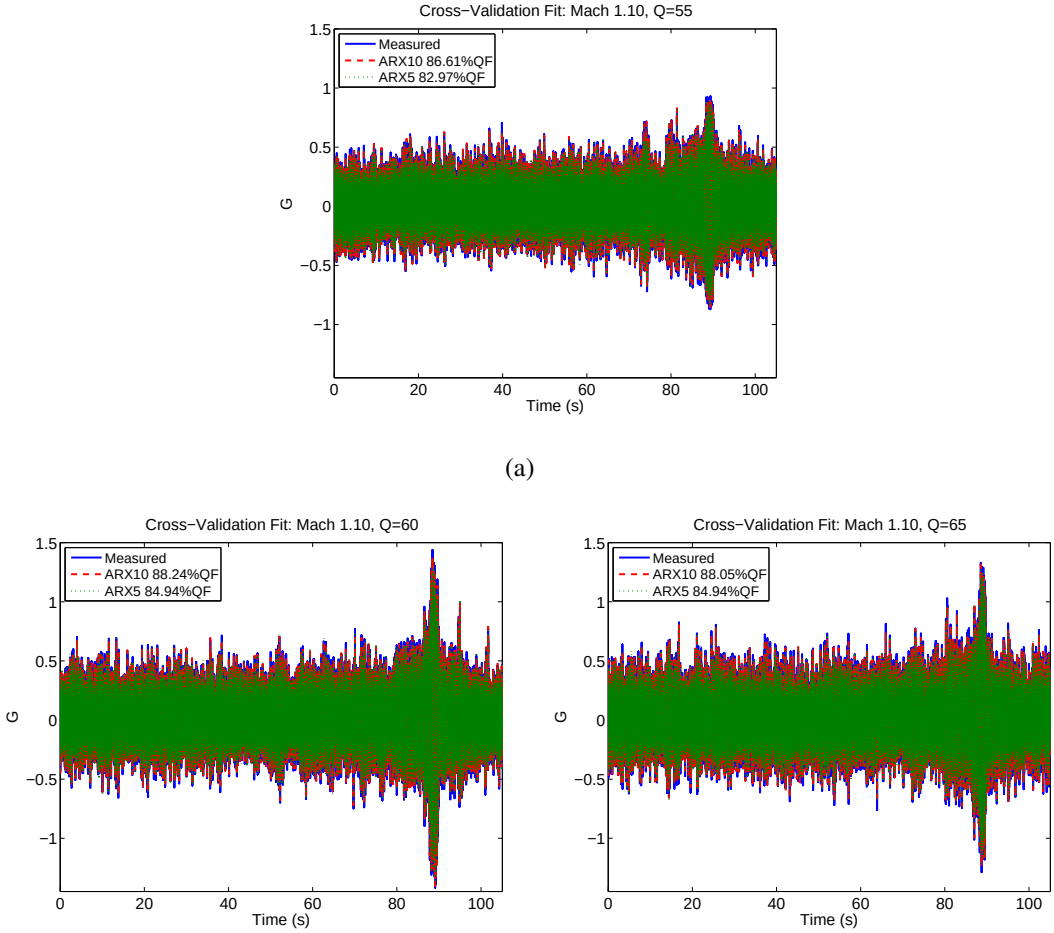

Figure 2: Measured and predicted output for ARX5 and ARX10 models at Mach 1.10. (a): $Q = 55$ psf. (b): $Q = 60$ psf. (c): $Q = 65$ psf. Solid line ("—") measured output. Dash-dash line ("– –") predicted ARX10 model output. Dot-dot line ("...") predicted ARX5 model output.

4.2 ARMAX Model

Next, we used the ARX10 model oder as a starting point to develop a more complex ARMAX model to assess whether it could account for more output variance whilst maintaining an efficient model description. The model was estimated at Mach 1.10, $Q = 30$ psf and yielded a structure of the form

$$\begin{aligned} &\text{ARMAX:} \\ \tilde{A}(q)y(n) &= \tilde{B}(q)u(n) + \tilde{C}(q)e(n) \quad \text{where} \\ \tilde{C}(q) &= 1 + \tilde{c}_1 q^{-1} + \tilde{c}_2 q^{-2} + \tilde{c}_3 q^{-3} + \tilde{c}_4 q^{-4} + \tilde{c}_5 q^{-5} \\ &+ \tilde{c}_6 q^{-6} + \tilde{c}_7 q^{-7} + \tilde{c}_8 q^{-8} + \tilde{c}_9 q^{-9} + \tilde{c}_{10} q^{-10}. \end{aligned} \tag{15}$$

Figure 3 shows representative results for the ARMAX structure's (Eqn.15) ability to represent S^{4}T wind-tunnel data by evaluating it with cross-validation data at Mach 1.10, Q =55, 60, 65 psf. The figure illustrates %QF of the predicted output for the ARMAX model superimposed on top of measured data. The %QF's obtained for the ARMAX model at Q =55, 60, 65 psf. are 87.38%, 88.86% and 88.67%, respectively. Notice that although this model structure adds complexity, it is accounts for incrementally more of the output variance.

4.3 Box-Jenkins Model

Lastly, we used the ARMAX model (Eqn. 15) oder as a starting point to develop a more complex BJ model to assess whether it could account for more output variance whilst maintaining an efficient model description. The model was estimated at Mach 1.10, $Q = 30$ psf and yielded a structure of the form

$$\begin{aligned} &\text{BJ:} \\ y(n) &= \frac{\tilde{B}(q)}{\tilde{F}(q)}u(n) + \frac{\tilde{C}(q)}{\tilde{D}(q)}e(n) \quad \text{where} \\ \tilde{F}(q) &\simeq \tilde{A}(q) \quad \text{and} \\ \tilde{D}(q) &= 1 + \tilde{d}_1 q^{-1} + \tilde{d}_2 q^{-2} + \tilde{d}_3 q^{-3} + \tilde{d}_4 q^{-4} + \tilde{d}_5 q^{-5} \\ &+ \tilde{d}_6 q^{-6} + \tilde{d}_7 q^{-7} + \tilde{d}_8 q^{-8} + \tilde{d}_9 q^{-9} + \tilde{d}_{10} q^{-10}. \end{aligned} \tag{16}$$

Figure 4 shows representative results for the BJ structure's (Eqn. 16) ability to represent S^{4}T wind-tunnel data by evaluating it with cross-validation data at Mach 1.10, Q =55, 60, 65 psf.

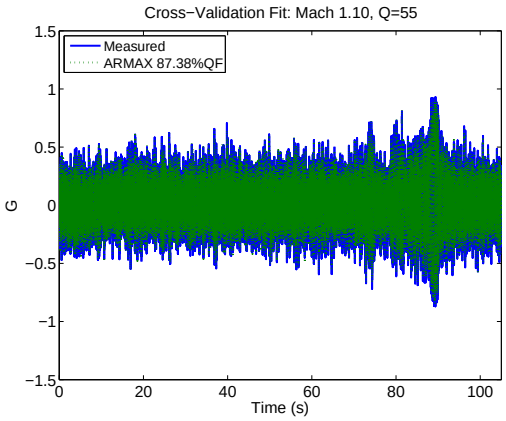

(a)

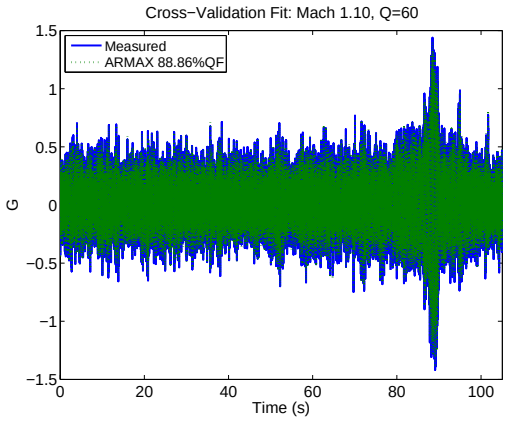

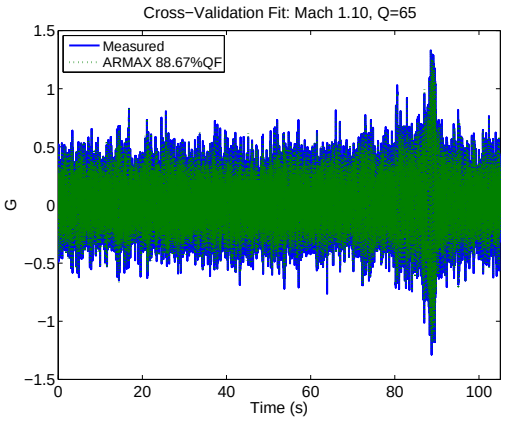

(b) (c)

Figure 3: Measured and predicted output for ARMAX model at Mach 1.10. (a): $Q = 55$ psf. (b): $Q = 60$ psf. (c): $Q = 65$ psf. Solid line ("—") measured output. Dot-dot line ("...") predicted ARMAX model output.

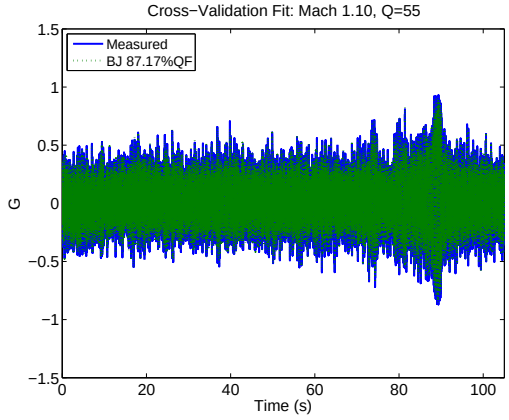

(a)

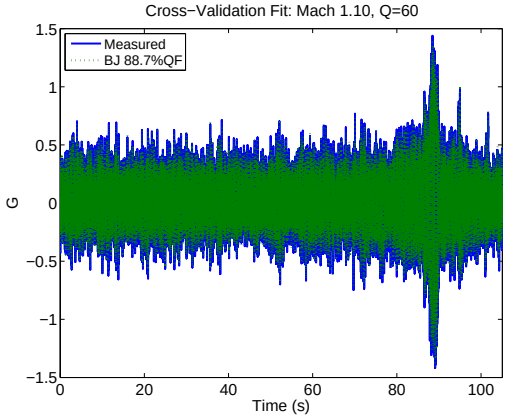

(b)

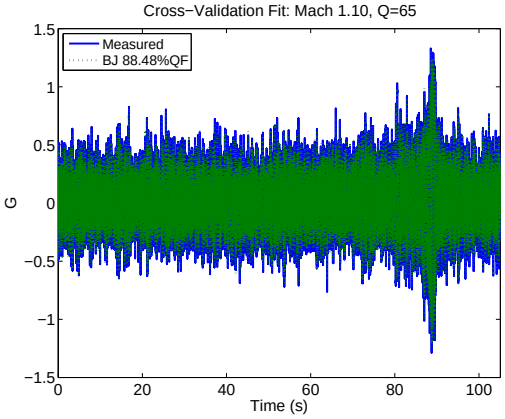

(c)

Figure 4: Predicted output of the BJ model at Mach 1.10 superimposed on top of measured output. (a): $Q = 55$ psf. (b): $Q = 60$ psf. (c): $Q = 65$ psf. Solid line ("—") measured output. Dot-dot line ("...") predicted BJ model output.

The figure illustrates %QF of the predicted output for the BJ model superimposed on top of measured data. The %QF's obtained for the BJ model at Q =55, 60, 65 psf. are 87.17%, 88.70% and 88.48%, respectively. Although the BJ model offers greater complexity to model the observed data, it offers a slightly lower %QF. Using validation data, if the fit of a higher order deteriorates, it is an indication that the model complexity is too high [33].

Table 1 summarises the findings of our analysis. These results from Table 1 illustrate that model

	Dynamic	Quality of Fit (%)			
Mach	Pressure (psf)	ARX5	ARX10	ARMAX	BJ
0.80	55	86.04	87.63	88.26	88.05
	60	86.81	88.25	88.87	88.61
	65	86.16	87.33	87.79	87.66
0.95	55	83.31	85.56	86.80	86.05
	60	83.60	85.97	87.11	86.36
	65	×	×	×	×
1.10	55	82.97	86.61	87.38	87.17
	60	84.94	88.24	88.86	88.70
	65	84.94	88.05	88.67	88.48

Table 1: Summary of cross-validation results. Mach number and dynamic pressure versus model structure.

fit increases with added complexity for the ARX model structure, improves incrementally for the ARMAX structure but decreases for the BJ. From these results we conclude that the higher-order ARX model may be sufficient for our purposes and as such we compare the predictive capability of this model to the FE based ASE model used for control design during wind-tunnel test [38, 39].

4.4 Comparison of Tenth-Order ARX and ASE Models

Lastly, we compared the ARX10 (Eqn. 14) and ASE model's ability to predict measured data. The original FE based model had 17,196 degrees of freedom. Using a modal approach an eightieth-order ASE model was developed and used for comparison [38, 39]. The ASE model

contained 60 structural and 20 unsteady aerodynamic lag states.

Figure 5 illustrates results of how accurately, as %QF, the two models correspond to wind-tunnel data at Mach 0.80, 0.95, 1.1 and, Q =55, 60, 65 psf. The figure shows the predicted output for

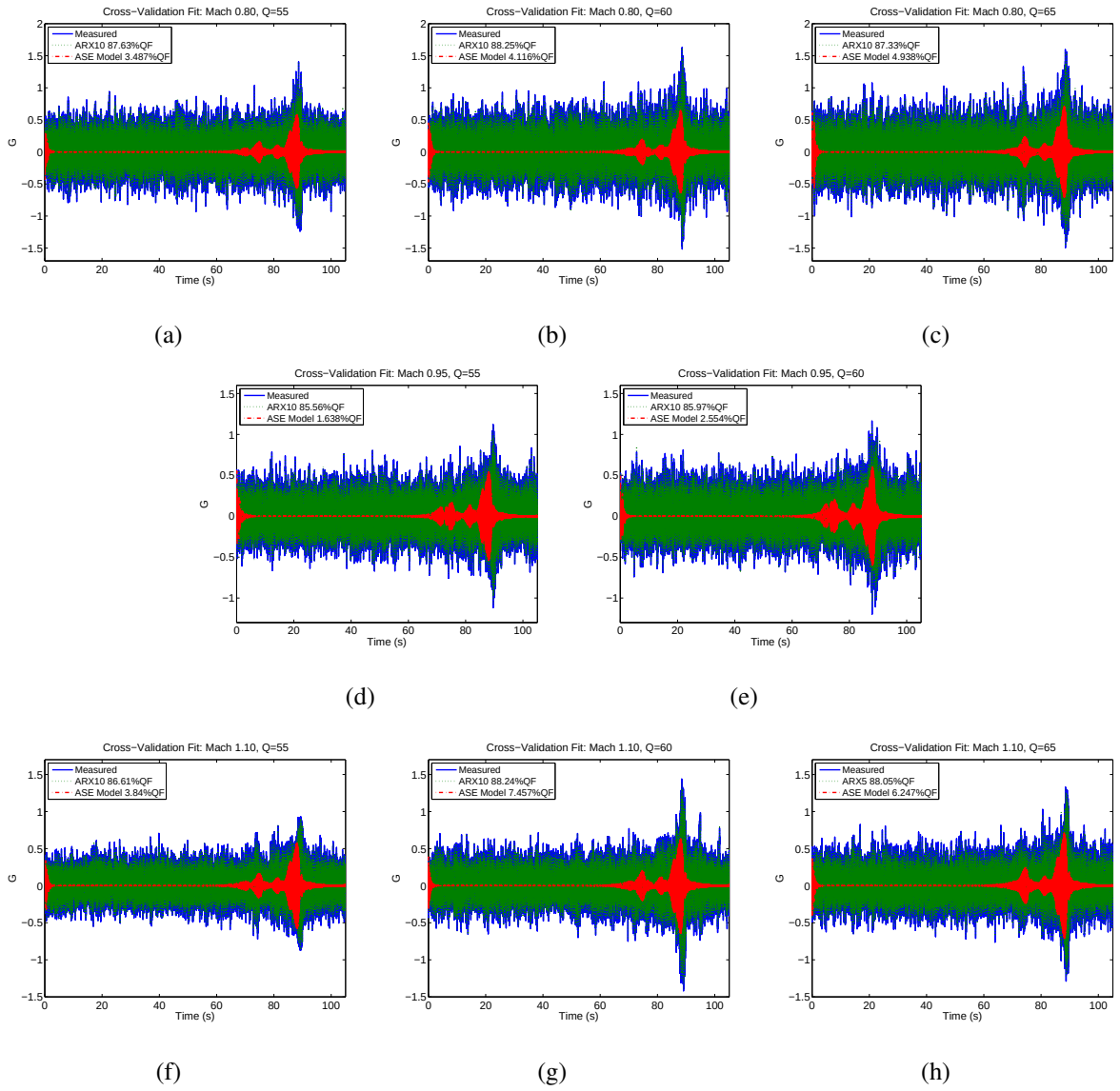

Figure 5: Predicted outputs of the ASE and ARX10 model superimposed on top of measured output. (a–c): Mach 0.80, $Q = 55 - 65$ psf. (d–e): Mach 0.95, $Q = 55 - 60$ psf. (c): Mach 1.10, $Q = 55 - 65$ psf. Solid line ("—") measured output. Dot-dot line ("...") predicted ARX10 model output. Dash-dot line ("–..") predicted ASE model output.

the ARX10 and ASE models superimposed on top of measured data. The %QF's obtained for the ARX10 model, at all Mach numbers and Q's, ranges from 85% to 88%. For the ASE model the %QF's, for all Mach numbers and Q's, ranges from 2% to 7%. Although the FE ASE has many more degrees of freedom, it was not able to provide better predictive capability

than the data-driven ARX model. Clearly, the tenth-order ARX model obtained using system identification methodology outperforms the FE ASE model.

5 DISCUSSION

This study explored the utility of system identification techniques to develop robust models for control synthesis. Initially, at each Mach number, an ARX model with maximum order of five was posed to the AIC, FPE and MDL techniques to estimate optimal lag and dynamic order. Next the ARX models were allowed greater flexibility with a maximum order of ten to assess whether the same structure could explain more of the output variance. Analysis of these results indicated that the tenth-order ARX models provided sufficient improvement in model fit to justify the added complexity. Therefore, at each Mach number the tenth-order ARX models were used as a starting point for ARMAX model development. The best fit ARMAX models were then used to develop BJ models.

The results show that whilst the ARMAX models provide an improved fit, it was less than 1% for each case. The predictive capability of the BJ models was less than that of the ARMAX structures, which is a symptom of too much complexity. As such, these results indicate that the tenth-order ARX models were optimal in terms of parsimony and predictive capability to describe the dynamics of recoded wind-tunnel data.

A comparison of the tenth-order ARX and 80th-order ASE model's ability to explain the output variance revealed that the more complex ASE model was not able to achieve as high of a fit. The ARX model was able to attain a higher fit because the model was developed using measured data which often contains dynamics that are not captured in a FE based model. Conversely, the ASE model was developed from idealised assumptions about mass, damping, etc. which are idealisation and often do not closely hold with observations under experimental conditions.

Although a different ASE model was developed for each Mach and Q, they yielded significantly reduced fits to measured data compared with the tenth-order ARX model. Notice that the ARX model at each Mach number was developed with estimation data at $Q = 30$ psf but was able to accurately predict the measured data at higher Q's, namely, $Q = 55 - 65$ psf. This is the power of utilising a data-driven approach to model development.

Often a model which yields a minimum system description yet provides good predictive ca-

pabilities is deemed as the best or optimal model. This is a trade-off between the ability to describe the system behaviour and parsimony. If two models can describe the system behaviour almost equally well, why choose the more complex one? For example, in H_∞-control synthesis the order of the controller is equal to the order of the model plus the order of the performance weights. Of course, it is not as computationally demanding to compute a controller of lower order. Moreover, selecting a model with greater complexity may lead to numerical issues if the model order is too high. Hence, minimum complexity often renders control synthesis more tractable [33, 47].

A future study will utalise these data-driven models to develop control laws to assess model and controller design robustness. Initially, this study will be performed in a simulation environment but with data collected from the wind-tunnel tests described in this paper. The successful demonstration of this work may lead to comparison of the robustness of control law design based on the two approaches, FE ASE and system identification models, on a supersonic flight test vehicle.

6 CONCLUSION

This study demonstrates the application of system identification techniques to develop parsimonious and robust models directly from data with excellent predictive capability. The results show that a data-driven model is capable of predicting observed data for a larger operating point. This robust predictive power was demonstrated with models developed at $Q = 30$ psf yet able to accurately predict the measured output at higher Q's. This superior predictive capability allows for simpler control solutions and reduced modelling effort whilst traditional ASE based control strategies rely on computationally expensive models with little predictive power rendering control law design more expensive.

ACKNOWLEDGMENTS

The author would like to thank Dr. Walter A. Silva and Dr. Boyd Perry III of NASA Langley Research Center for providing the data for this study.

7 REFERENCES

[1] Danowsky, B., Thompson, P., Farhat, C., et al. (2008). Residualization of an aircraft linear aeroelastic reduced order model to obtain static stability derivatives. In *6th AIAA*

Atmospheric Flight Mechanics Conference and Exhibit. Honolulu HI, pp. AIAA 2008–6370.

[2] Courant, R. (1943). Variational methods for the solution of problems of equilibrium and vibrations. *Bulletin of the American Mathematical Society*, 49(1), 1–23.

[3] Hrennikoff, A. (1941). Solution of problems of elasticity by the frame-work method. *Journal of Applied Mechanics*, 8, A169–A175.

[4] King, B., Hovakimyan, N., Evans, K., et al. (2006). Reduced order controllers for distributed parameter systems: LQG balanced truncation and an adaptive approach. *Mathematical and Computer Modelling*, 43, 1136–1149.

[5] Karhunen, K. (1946). Zur spektraltheorie stochastischer prozesse. *Annales Academiae Scientiarum Fennicae*, 37.

[6] Ahmed, N. and Rao, K. (1975). *Orthogonal Transforms for Digital Signal Processing*. New York: Springer-Verlag.

[7] Almroth, B., Stern, P., and Brogan, F. (1978). Automatic choice of global shape functions in structural analysis. *AIAA Journal*, 16(5), 525–528.

[8] Nagy, D. (1979). Modal representation of geometrically nonlinear behavior by the finite element method. *Computers & Structures*, 10(4), 683–688.

[9] Lucia, D., King, P., and Beran, P. (2003). Reduced order modeling of a two-dimensional flow with moving shocks. *Computers & Fluids*, 32(7), 917–938.

[10] Noor, A. and Peters, J. (1983). Recent advances in reduction methods for instability analysis of structures. *Computers & Structures*, 16(1), 67–80.

[11] Noor, A., Peters, J., and Andersen, C. (1981). Reduced basis technique for collapse analysis of shells. *AIAA Journal*, 19(3), 393–397.

[12] May, S. and Smith, R. (2009). Reduced-order model design for nonlinear smart system models. In *Modeling, Signal Processing, and Control for Smart Structures*, vol. 7286.

[13] Banks, H., Beeler, S., Kepler, G., et al. (2002). Reduced order modeling and control of thin film growth in an HPCVD reactor. *SIAM Journal on Applied Mathematics*, 62(4), 1251–1280.

[14] Fukunaga, K. (1990). *Introduction to Statistical Recognition*. New York: Academic Press.

[15] Holmes, P., Lumley, J., and Berkooz, G. (1996). *Turbulence, Coherent Structures, Dynamical Systems and Symmetry*. Cambridge Monographs on Mechanics. Cambridge University Press.

[16] Ito, K. and Schroeter, J. D. (2001). Reduced order feedback synthesis for viscous incompressible flows. *Mathematical and Computer Modelling*, 33(1), 173–192.

[17] Sirovich, L. (1987). Turbulence and the dynamics of coherent structures. *Quarterly of Applied Mathematics*, 45(10), 561–590.

[18] Ly, H. and Tran, H. (2001). Modelling and control of physical processes using proper orthogonal decomposition. *Mathematical and Computer Modelling*, 33(1), 223–236.

[19] Shvartsman, S. and Kevrikidis, I. (1998). Nonlinear model reduction for control of distributed parameter systems: a computer-assisted study. *AIChE Journal*, 44(7), 1579–1595.

[20] Graham, W., Peraire, J., and Tang, K. (1999). Optimal control of vortex shedding using low-order models. *International Journal for Numerical Methods in Engineering*, 44(7), 973–990.

[21] Du, H., Zhang, N., and Nguyen, H. (2008). Mixed H_2/H_∞ control of tall buildings with reduced-order modelling technique. *Structural Control and Health Monitoring*, 15(1), 64–89.

[22] Banks, H., Joyner, M., Winchesky, B., et al. (2000). Nondestructive evaluation using a reduced-order computational methodology. *Inverse Problems.*, 16(4), 929–945.

[23] Lucia, D., Beran, P., and Silva, W. (2004). Reduced-order modeling: new approaches for computational physics. *Progress in Aerospace Sciences*, 40(1), 51–117.

[24] Romanowski, M. (1996). Reduced order unsteady aerodynamic and aeroelastic models using karhunen-loeve eigenmodes. In *6th AIAA/USAF/NASA/ISSMO Symposium on Multidisciplinary Analysis and Optimization*. Bellevue WA, pp. 7–13.

[25] Kim, T. (1998). Frequency-domain Karhunen-Loeve method and its application to linear dynamic systems. *AIAA Journal*, 36(11), 2117–2123.

[26] Hall, K., Thomas, J., and Dowell, E. (2000). Proper orthogonal decomposition technique for transonic unsteady aerodynamic flows. *AIAA Journal*, 38(10), 1853–1862.

[27] Pettit, C. and Beran, P. (2000). Reduced-order modeling for flutter prediction. In *41st AIAA/ASCE/AHS/ASC Structures, Structural Dynamics, and Materials Conference and Exhibit*. Atlanta, GA, pp. AIAA–2000–1446.

[28] Pettit, C. and Beran, P. (2002). Application of proper orthogonal decomposition to the discrete Euler equations. *International Journal for Numerical Methods in Engineering*, 55(4), 479–497.

[29] Dowell, E., Thomas, J., and Hall, K. (2004). Transonic limit cycle oscillation analysis using reduced order aerodynamic models. *Journal of Fluids and Structures*, 19(1), 17–27.

[30] Cardoso, M., Durlofsky, L., and Sarma, P. (2009). Development and application of reduced-order modeling procedures for subsurface flow simulation. *International Journal for Numerical Methods in Engineering*, 77(9), 1322–1350.

[31] Cardoso, M. and Durlofsky, L. (2010). Linearized reduced-order models for subsurface flow simulation. *Journal of Computational Physics*, 229(3), 681–700.

[32] Rewienski, M. and White, J. (2003). A trajectory piecewise-linear approach to model order reduction and fast simulation of nonlinear circuits and micromachined devices. *IEEE Transactions on ComputerAided Design of Integrated Circuits and Systems*, 22(2), 155–170.

[33] Ljung, L. (1999). *System Identification: Theory for the User*. Upper Saddle River, New Jersey: Prentice Hall, Inc., second ed.

[34] Bendat, J. S. and Piersol, A. G. (1986). *Random Data: Analysis and measurement procedures*. New York: Johns Wiley and Sons, second ed.

[35] Siebert, W. M. (1986). *Circuits, Signals, and Systems*. Cambridge, Massachusetts: The MIT Press, first ed.

[36] Chen, R. and Tsay, R. (1993). Nonlinear additive ARX models. *Journal of the American Statistical Association*, 88(423), 955–967.

[37] Perry, I., B, Silva, W. A., Florance, J. R., et al. (2007). Plans and status of wind-tunnel testing employing an aeroservoelastic semispan model. In *48th AIAA/ASME/ASCE/AHS/ASC Structures, Structural Dynamics, and Materials Conference*. Honolulu, Hawaii, pp. AIAA–2007–1770.

[38] Chen, P., Moulin, B., Ritz, E., et al. (2009). CFD-based aeroservoelastic control for supersonic flutter suppression, gust load alleviation, and ride quality enhancement. In *50th AIAA/ASME/ASCE/AHS/ASC Structures, Structural Dynamics, and Materials Conference*. Palm Springs, California, pp. AIAA–2009–2537.

[39] Moulin, B., Ritz, E., Chen, P., et al. (2010). CFD-based control for flutter suppression, gust load alleviation, and ride quality enhancement for the S^4T. In *51st AIAA/ASME/ASCE/AHS/ASC Structures, Structural Dynamics, and Materials Conference*. Orlando, Florida, pp. AIAA 2010–2623.

[40] Goodwin, G. and Payne, R. (1977). *Dynamic System Identification: Experiment Design and Data Analysis*, vol. 136 of *Mathematics in Science and Engineering*. New York: Academic Press.

[41] Hsia, T. C. (1977). *System Identification: Least-Squares Methods*. Lexington, Massachusetts: Lexington Books, D.C. Heath and Company.

[42] Box, G. and Jenkins, G. (1970). *Time series analysis: Forecasting and control*. San Francisco: Holden-Day, first ed.

[43] Akaike, H. (1969). Fitting autoregressive models for prediction. *Annals of the Institute of Statistical Mathematics*, 21(1), 243–247.

[44] Akaike, H. (1974). A new look at the statistical model identification. *IEEE Transactions on Automatic Control*, 19(6), 716–723.

[45] Rissanen, J. (1978). Modelling by shortest data description. *Automatica*, 14, 465–471.

[46] Boulet, B. and Francis, B. (1998). Consistency of open-loop experimental frequency-response data with coprime factor plant models. *IEEE Transactions on Automatic Control*, 43(12), 1680–1691.

[47] Zhou, K., Doyle, J. C., and Glover, K. (1995). *Robust & Optimal Control*. Upper Saddle River, New Jersey: Prentice Hall PTR, first ed.

Data Driven Model Development for the SuperSonic SemiSpan Transport (S^4T)

Sunil L. Kukreja
NASA, Dryden Flight Research Center
Edwards, California, USA

Outline

- Introduction
- Objectives
- System Identification
- Identification Procedure
- Results
- Conclusions

Introduction

- Undesirable ASE interactions are a major concern in modern aircraft design
  - ASE interactions between aircraft structure, aerodynamics and flight control systems can lead to divergent oscillations resulting in catastrophic failure
  - Accurate models allow for robust control design – critical for aircraft safety, gust-load alleviation, ride quality, etc.
- Finite element (FE) based models used in design process of aircraft to aid in the description of complex elastic and structural components
  - FE based models that accurately characterise the aerodynamic and structural components are of very high order (e.g. thousands of degrees of freedom) and computationally intensive
- Led to considerable activity in the areas of model and controller reduction techniques – reduced order model (ROM) techniques

ROM Techniques

- Proper Orthogonal Decomposition (POD) (i.e. Karhunen-Loeve Procedure)
  - POD technique well known in statistical literature as principal-component analysis
  - Uses synthetic data from a high fidelity FE based model to capture the dominant characteristic information utilising an orthogonalisation process
- Trajectory Piecewise Linearisation (TPWL)
  - Developed because standard POD procedures less robust for nonlinear problems
  - TPWL technique combines reduced-order modelling with linearization of the governing equations as a solution to this problem
- ROM techniques offer significant reduction of full FE based model, however, often still too large for efficient control design
- An alternative approach is data driven techniques to let the data dictate what the optimal model should be – i.e. system identification

The Identification Problem

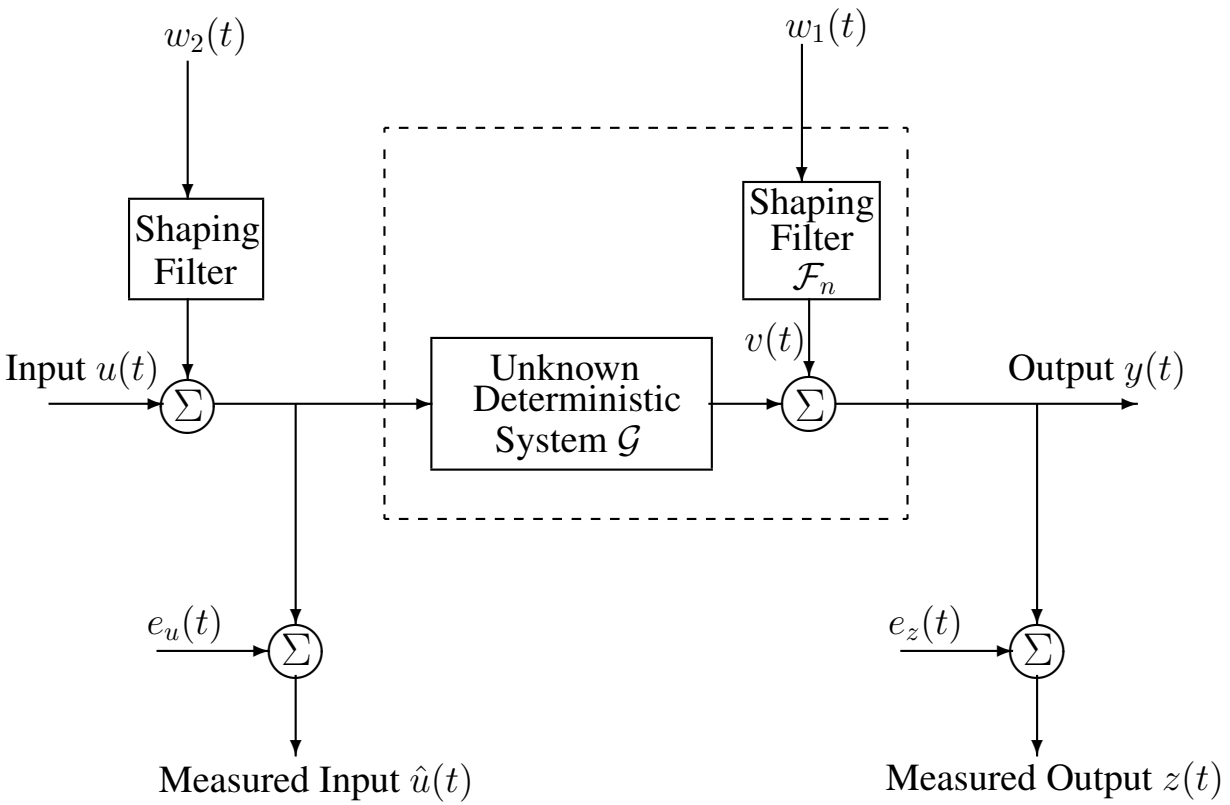

Identification of Stochastic or Noise Model

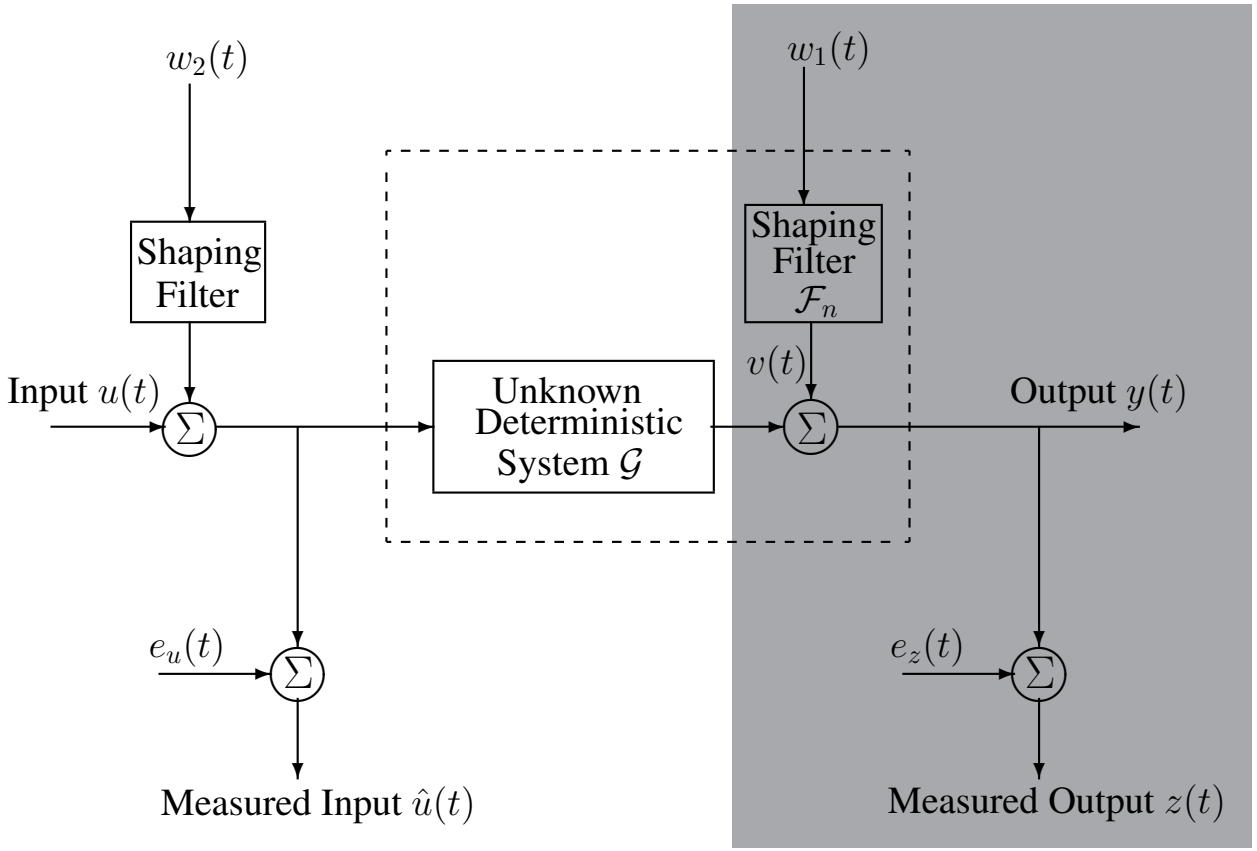

- Relationship between $w_1(t)$ and $z(t)$, given only system output, $z(t)$
- $u(t)$ assumed zero or constant
- Commonly known as time-series analysis
- Economic analysis, geophysical or astronomical phenomena, biological data

Identification of the Deterministic Model, $\mathcal{G}$

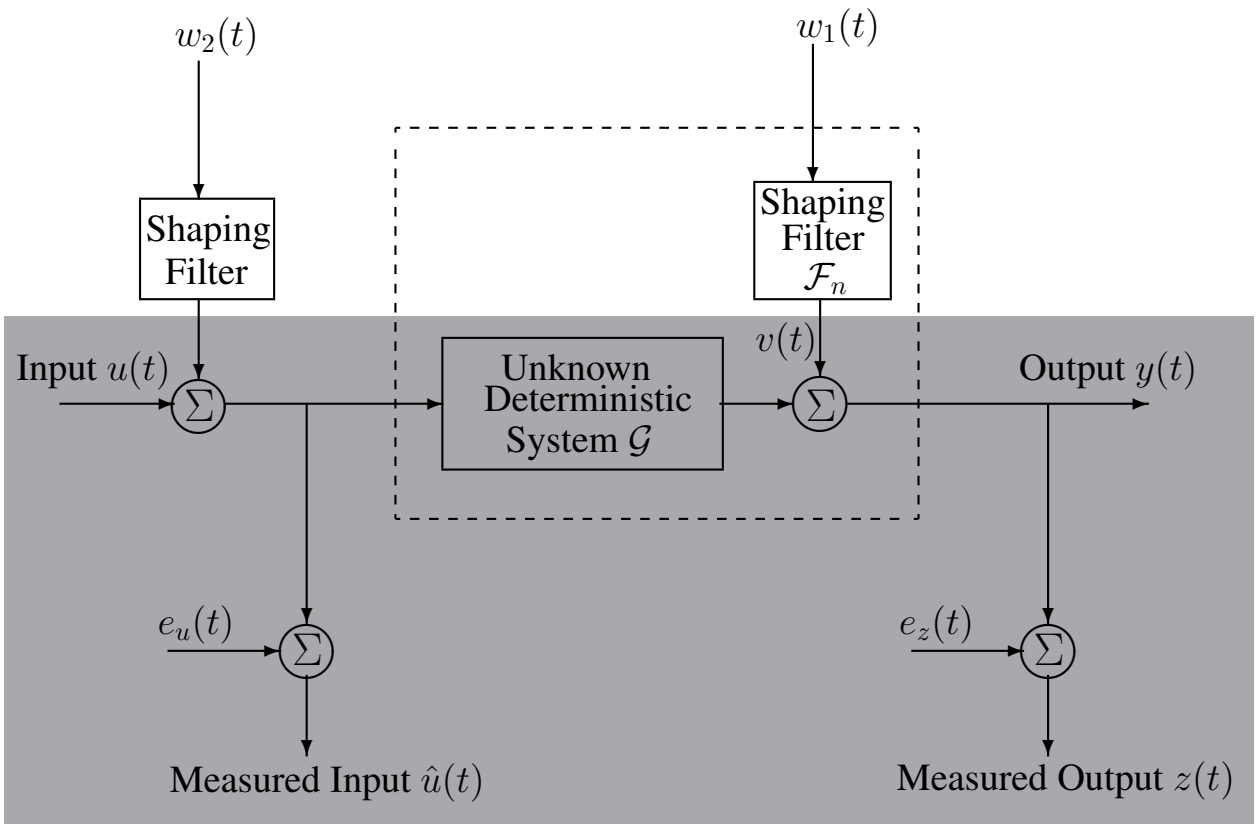

- Relationship between $u(t)$ and $y(t)$ – assumes $w_1(t) = 0$
- Input/output corrupted by noise, $e_u(t)$ & $e_z(t)$ – commonly assumes $e_u(t) = 0$
- Pursued when objective is to gain insight into the functioning of a system
- Automotive industry, chemical plants, pulp & paper, biomedical modelling

Identification of Stochastic & Deterministic Models

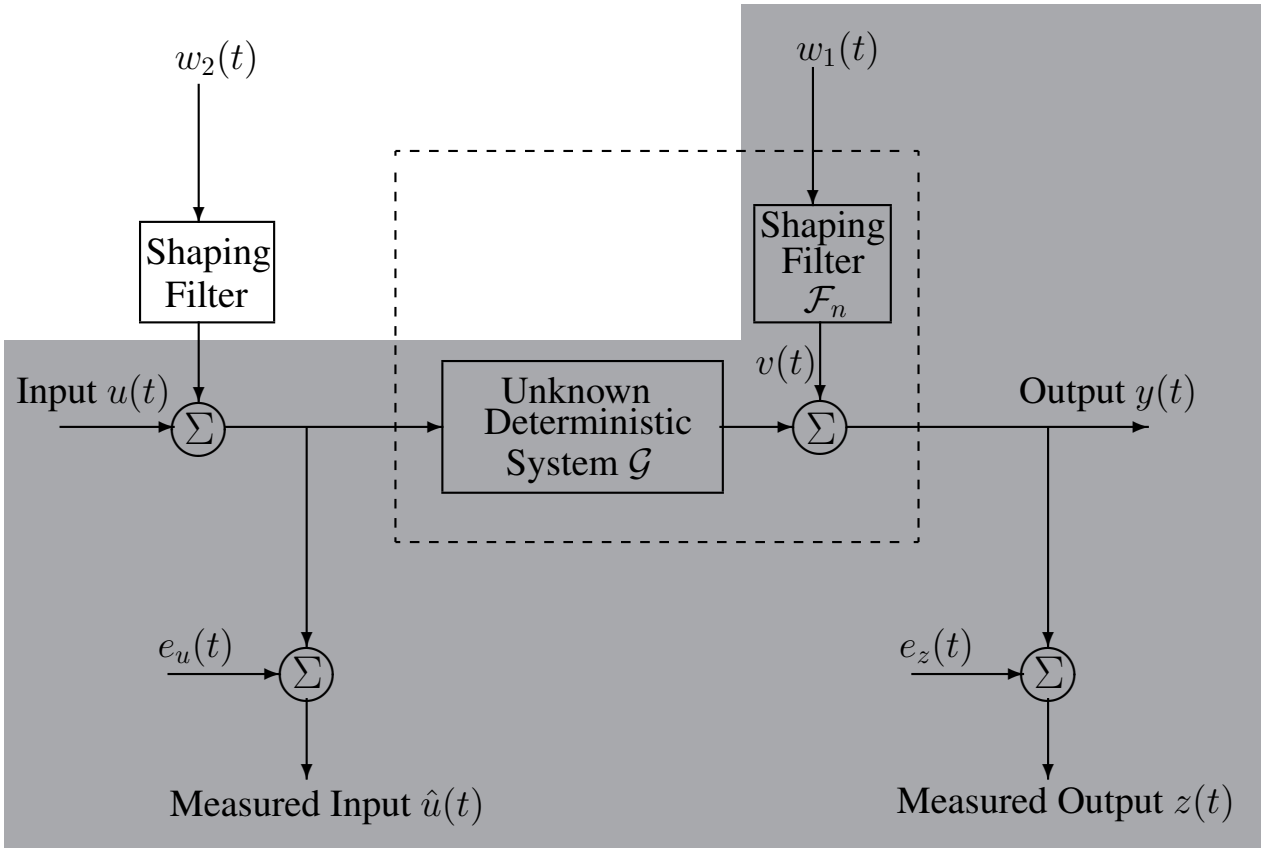

- Both input/output signals available for identification
- Used when accurate predictions are desired
- Design of model-based control systems for aircraft, spacecraft or robotics

Nonparametric Methods

- Advantage
  - Provide convenient, robust means of characterising the dynamics of systems without requiring a priori assumptions regarding the system structure

- Disadvantage
  - Nonparametric estimates of dynamics are difficult to relate to the structure and parameters of the underlying physiological system

Parametric Methods

- Disadvantage
  - Generally require a priori assumptions about the system order
- Advantage
  - Provides a concise description of the system dynamics
  - Yield results that may be related directly to the system structure

Objective

- Investigate two common approaches to model development for robust control synthesis in the aerospace community
- Reduced order aeroservoelastic modelling based on structural finite-element and computational fluid dynamics based aerodynamic models
- Data-driven system identification procedure

Identification Procedure

- Choose Model Structure
  - Determine model form and select parameters to include in a model
- Model Order Selection
  - Determine number of input, output and error lags
- Parameter Estimation
  - Determine values of unknown parameters
- Model Validation
  - Assess whether identified nominal model can reproduce data from a plant

Model Structures

- ARX Model

$$\begin{aligned} y(n) &= -a_1 y(n-1) - \cdots - a_{n_a} y(n-n_a) + b_1 u(n-1) + b_2 u(n-2) + \cdots + b_{n_b} u(n-n_b) \\ &\quad + e(n) \end{aligned}$$

$$y(n) = G(q)u(n) + H(q)e(n) \quad \text{where} \quad G(q) = \frac{B(q)}{A(q)}, \quad H(q) = \frac{1}{A(q)}$$

- ARMAX Model

$$\begin{aligned} y(n) &= -a_1 y(n-1) - \cdots - a_{n_a} y(n-n_a) + b_1 u(n-1) + b_2 u(n-2) + \cdots + b_{n_b} u(n-n_b) \\ &\quad + e(n) + c_1 e(n-1) + \cdots + c_{n_c} e(n-n_c) \end{aligned}$$

$$\text{where} \quad G(q) = \frac{B(q)}{A(q)}, \quad H(q) = \frac{C(q)}{A(q)}$$

- Box-Jenkins Model

$$y(n) = \frac{B(q)}{F(q)}u(n) + \frac{C(q)}{D(q)}e(n)$$

$$\text{where} \quad F(q) = 1 + f_1 q^{-1} + \cdots + f_{n_f} q^{-n_f} \quad \text{and} \quad D(q) = 1 + d_1 q^{-1} + \cdots + d_{n_d} q^{-n_d}$$

Model Order Selection

- Final Prediction Error (FPE)

$$\text{FPE} = V\left(1 + \frac{2p}{N-p}\right)$$

where N is the number of data points, V is the prediction error, or the residual sum of squares and p is the number of model parameters

- Akaike's Information Criterion (AIC)

$$\text{AIC} = V\left(1 + \frac{2p}{N}\right)$$

- Minimal Description Length (MDL)

$$\text{MDL} = V\left(1 + \frac{p \ln N}{N}\right)$$

Cross-Validation

- Model validation concerned with assessing whether a given nominal model can reproduce data from a plant, collected after some initial experiments to obtain estimation data

- Model goodness is assessed by

$$\%QF = \left(1 - \frac{\frac{1}{N}\sum_{n=1}^{N}(y_n - \hat{y}_n)^2}{\frac{1}{N}\sum_{n=1}^{N}(y_n)^2}\right) \times 100$$

Experimental S^{4}T Wind-Tunnel Data from NASA Langely Research Center

- Data analysed used horizontal tail position input and structural accelerometer response output

Data Collection

- Data recorded during transonic clearance
- Aircraft model was perturbed with a log sine sweep input and had a mean value of 3.5 deg and ± 0.3 deg amplitude
- Inputs applied to horizontal tail and output data collected from sensor located at nacelle inboard aft position
- Data was collected for $M = 0.6 - 1.2$ and dynamic pressures $Q = 20 - 65$ psf

Data Analysis

- Objective was to develop a parsimonious model for control synthesis to improve gust-load alleviation and ride quality
- Focused our identification efforts on data collected at Mach 0.80, 0.95, 1.10 and $Q = 30$, 55, 60, 65 psf
- Used $Q = 30$ psf as estimation data and $Q = 55, 60, 65$ psf as cross-validation data
- At $M = 0.95$ data was not collected at $Q = 65$ psf and, therefore, the estimated model could only be cross-validated at $Q = 55$ and 60 psf.

Identification Procedures

- Model order was estimated using FPE, AIC and MDL
- Prediction error identification (PEI) used to estimate unknown parameters
- Identification process was performed in four stages:
  1. ARX structure's ability to model wind-tunnel data assessed because it is the simplest input-output model and invoking the principle of parsimony. Model order determined by preselecting a search range of: n_a =2–5, n_b =1–5, n_k =1–10. Range selected to allow sufficient model complexity whilst maintaining an efficient system description.
  2. Complexity added to ARX model to assess whether the same model structure could account for significantly greater output variance with n_a =2–10, n_b =1–10, n_k =1–20.
  3. Using best fit ARX model order to fix n_a and n_b we searched for an ARMAX order, namely, n_c =1–20 that provided the smallest prediction error as the optimal order.
  4. The same procedure was followed to assess whether the BJ model structure could account for more of the output variance than the ARMAX model with n_d =1–20.

Results: ARX Model....

- Two ARX model orders evaluated: n_a =5, n_b =1, n_k =1 and n_a =10, n_b =1, n_k =1 with estimation data from Mach1.10, $Q = 30$ psf

ARX5:

$$\begin{aligned}
\hat{A}(q)y(n) &= \hat{B}(q)u(n) + e(n) \quad \text{where} \\
\hat{A}(q) &= 1 + \hat{a}_1 q^{-1} + \hat{a}_2 q^{-2} + \hat{a}_3 q^{-3} + \hat{a}_4 q^{-4} + \hat{a}_5 q^{-5} \quad \text{and} \\
\hat{B}(q) &= \hat{b}_1 q^{-1}
\end{aligned}$$

ARX10:

$$\begin{aligned}
\tilde{A}(q)y(n) &= \tilde{B}(q)u(n) + e(n) \quad \text{where} \\
\tilde{A}(q) &= 1 + \tilde{a}_1 q^{-1} + \tilde{a}_2 q^{-2} + \tilde{a}_3 q^{-3} + \tilde{a}_4 q^{-4} + \tilde{a}_5 q^{-5} \\
&+ \tilde{a}_6 q^{-6} + \tilde{a}_6 q^{-6} + \tilde{a}_6 q^{-6} + \tilde{a}_6 q^{-6} + \tilde{a}_{10} q^{-10} \quad \text{and} \\
\tilde{B}(q) &= \tilde{b}_1 q^{-1}.
\end{aligned}$$

....Results: ARX Model Cross-Validation at Mach 1.10, Q =55, 60, 65 psf

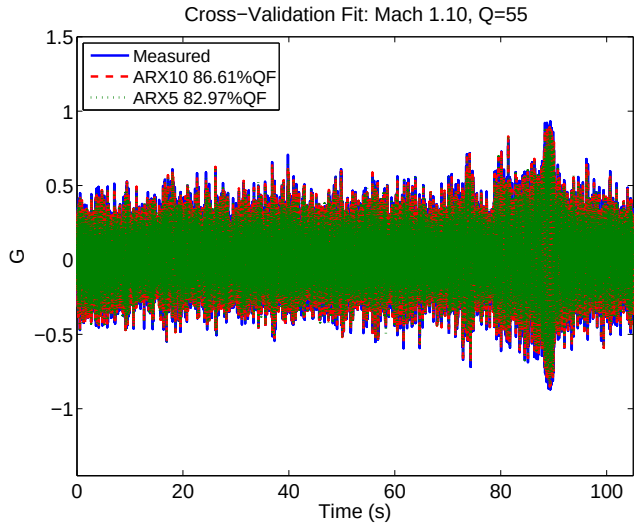

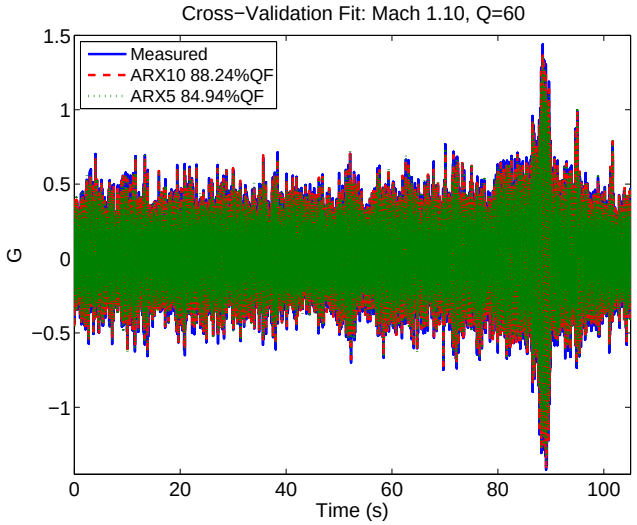

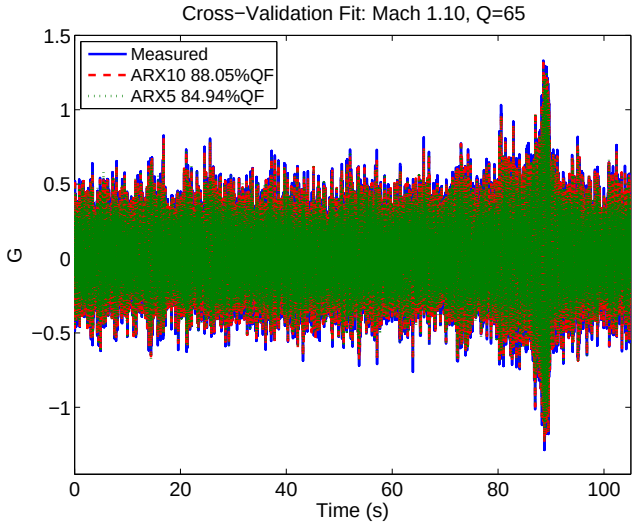

Results: ARMAX Model....

- Used the ARX10 model order as a starting point to develop a more complex ARMAX model with estimation data from Mach1.10, $Q = 30$ psf

ARMAX:

$$\begin{aligned} \tilde{A}(q)y(n) &= \tilde{B}(q)u(n) + \tilde{C}(q)e(n) \quad \text{where} \\ \tilde{C}(q) &= 1 + \tilde{c}_1 q^{-1} + \tilde{c}_2 q^{-2} + \tilde{c}_3 q^{-3} + \tilde{c}_4 q^{-4} + \tilde{c}_5 q^{-5} \\ &+ \tilde{c}_6 q^{-6} + \tilde{c}_7 q^{-7} + \tilde{c}_8 q^{-8} + \tilde{c}_9 q^{-9} + \tilde{c}_{10} q^{-10}. \end{aligned}$$

....Results: ARMAX Model

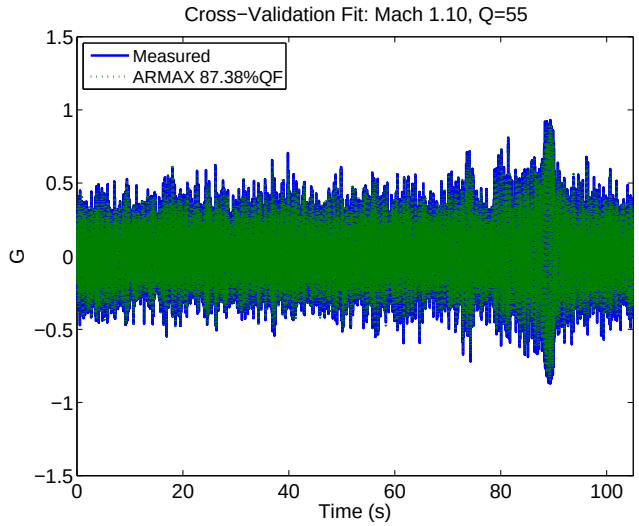

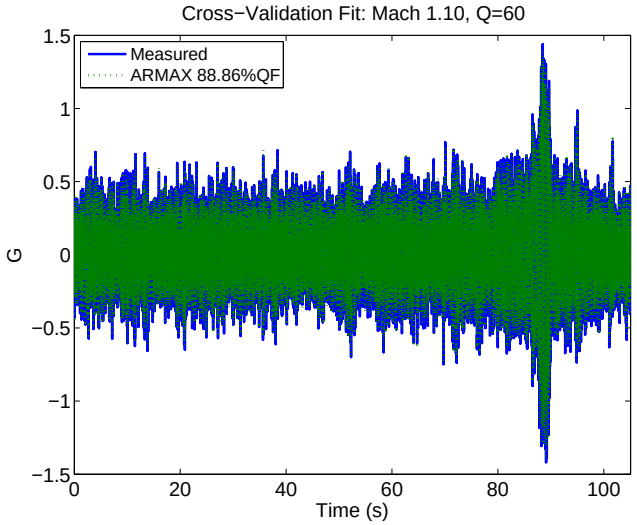

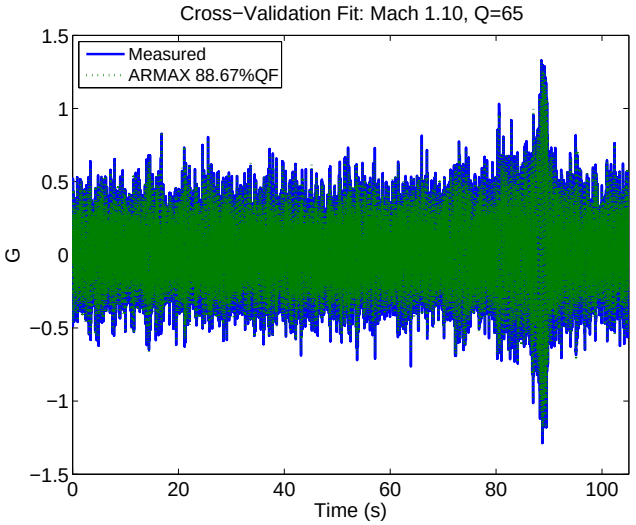

Results: Box-Jenkins Model....

- Used the ARMAX model order as a starting point to develop a more complex BJ model with estimation data from Mach1.10, $Q = 30$ psf

BJ:

$$
\begin{aligned}
y(n) &= \frac{\tilde{B}(q)}{\tilde{F}(q)}u(n) + \frac{\tilde{C}(q)}{\tilde{D}(q)}e(n) \quad \text{where} \\
\tilde{F}(q) &\simeq \tilde{A}(q) \quad \text{and} \\
\tilde{D}(q) &= 1 + \tilde{d}_1 q^{-1} + \tilde{d}_2 q^{-2} + \tilde{d}_3 q^{-3} + \tilde{d}_4 q^{-4} + \tilde{d}_5 q^{-5} \\
&+ \tilde{d}_6 q^{-6} + \tilde{d}_7 q^{-7} + \tilde{d}_8 q^{-8} + \tilde{d}_9 q^{-9} + \tilde{d}_{10} q^{-10}.
\end{aligned}
$$

....Results: Box-Jenkins Model

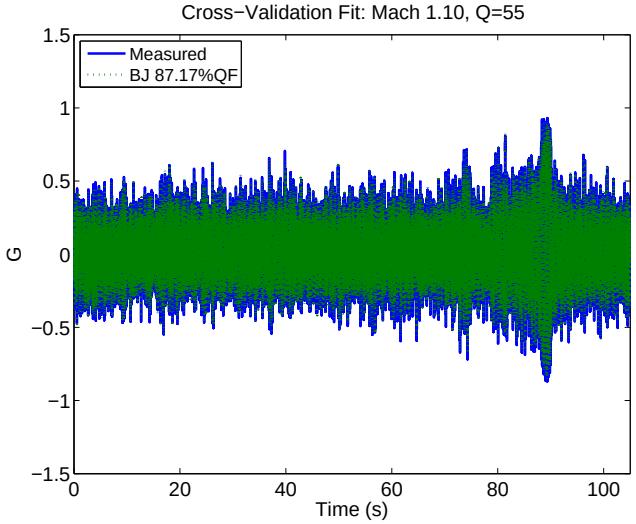

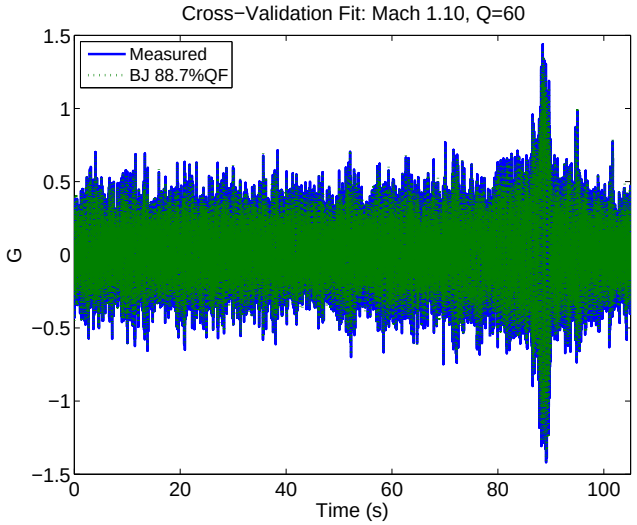

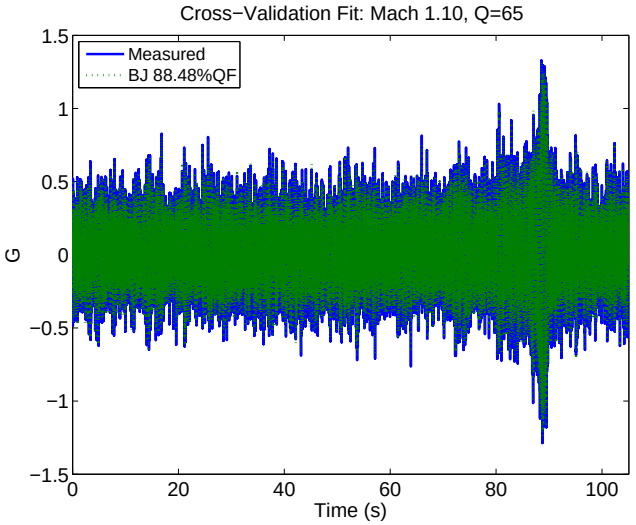

Summary of Cross-Validation: Mach & Dynamic Pressure Vs. Model

- Results illustrate that model fit increases with added complexity for the ARX model structure, improves incrementally for the ARMAX structure but decreases for the BJ

- We conclude that the higher-order ARX model may be sufficient for our purposes and as such we compare the predictive capability of this model to the FE based ASE model used for control design during wind-tunnel test

Comparison of Tenth-Order ARX and ASE Models

- Compared the ARX10 and ASE model's ability to predict measured data
- FE based model had 17,196 degrees of freedom, using a modal approach an eightieth-order ASE model was developed and used for comparison
- ASE model contained 60 structural and 20 unsteady aerodynamic lag states

Predicted Outputs of ASE, ARX10 Models Measured Output

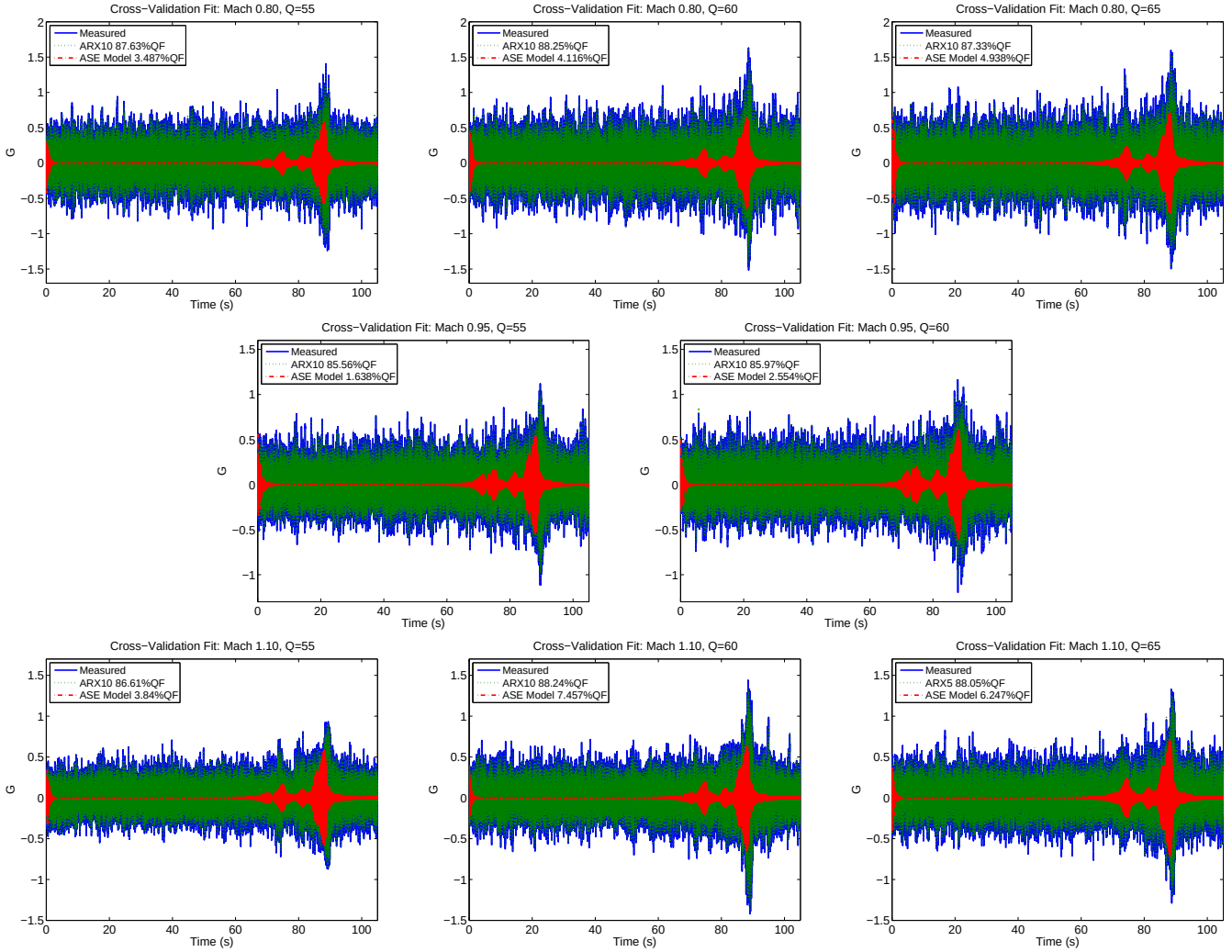

Conclusions

- Study demonstrates the application of system identification techniques to develop parsimonious and robust models directly from data with excellent predictive capability

- Results show that a data-driven model is capable of predicting observed data for a larger operating poin

- Robust predictive power was demonstrated with models developed at $Q = 30$ psf yet able to accurately predict the measured output at higher Q's

- Superior predictive capability allows for simpler control solutions and reduced modelling effort whilst traditional ASE based control strategies rely on computationally expensive models with little predictive power rendering control law design more expensive

Acknowledgments

The author would like to thank Dr. Walter A. Silva and Dr. Boyd Perry III of NASA Langley Research Center for providing the data for this study.